Design considerations for a C-shaped PET system, dedicated to small animal brain imaging, using GATE Monte Carlo simulations

N Efthimiou[1], P Papadimitroulas[2], T Kostou[2], G Loudos[1]
[1] Department of Biomedical Engineering, Technological Educational Institute of Athens, Greece.
[2] Department of Medical Physics, School of Medicine, University of Patras, Greece.

E-mail: efthimioun@upatras.gr

Abstract. Commercial clinical and preclinical PET scanners rely on the full cylindrical geometry for whole body scans as well as for dedicated organs. In this study we propose the construction of a low cost dual-head C-shaped PET system dedicated for small animal brain imaging. Monte Carlo simulation studies were performed using GATE toolkit to evaluate the optimum design in terms of sensitivity, distortions in the FOV and spatial resolution. The PET model is based on SiPMs and BGO pixelated arrays. Four different configurations with C-angle 0^o, 15^o, 30^o and 45^o within the modules, were considered. Geometrical phantoms were used for the evaluation process. STIR software, extended by an efficient multi-threaded ray tracing technique, was used for the image reconstruction. The algorithm automatically adjusts the size of the FOV according to the shape of the detector's geometry. The results showed improvement in sensitivity of ~15% in case of 45^o C-angle compared to the 0^o case. The spatial resolution was found 2 mm for 45° C-angle.

1. Introduction

Nowadays, most clinical and preclinical PET scanners rely on the cylindrical or near-cylindrical geometry [1-5]. Yet, there are some implementations which are based on alternative geometries such as rotating [6-9] or static planar heads [10-12]. The incorporation of SiPM arrays provides the means to design flexible PET scanners so as to improve sensitivity, with limited number of detector heads [13]. The design and configuration, of such systems, strongly depends on the particular region under investigation, but the driving factors are to maximize sensitivity and lower the cost [14].

In this study we evaluated the performance of a design for a C-shaped PET scanner designed for small animal brain imaging. We tried to incorporate the minimum amount of detectors, in order to keep the cost as low as possible. The designs were evaluated in terms of sensitivity, distortions in the FOV and spatial resolution.

2. Material and Methods

2.1. GATE simulations

We used the GATE (v.7) simulation toolkit to perform the simulations [15]. The geometry was based on a realistic hypothesis of six modules of a 6×6 BGO array [16], with crystal size 2.0×2.0×0.5 mm^3

coupled to SiPM arrays (1.35×1.35 mm^2). Each, head is assembled from 3 modules, which can be tilted, with respect to the central module, forming the C-shape. The head separation distance was defined as the distance between the central detector modules of each head. In this experimental setup was set to 3 cm.

In order to evaluate the effect of the C-angle to the performance of the system, four configurations of 0°, 15°, 30° and 45° C-angle, were considered. The configurations are illustrated in Figure 1. The size of the FOV and thus of the reconstructed images depends on the C-angle and was 59×59, 52×52, 48×48 and 44×44 pixels for 0°, 15°, 30° and 45° C-angle, respectively.

After the simulations a 400-650keV energy window, was applied. Random and scattered corrections were not considered.

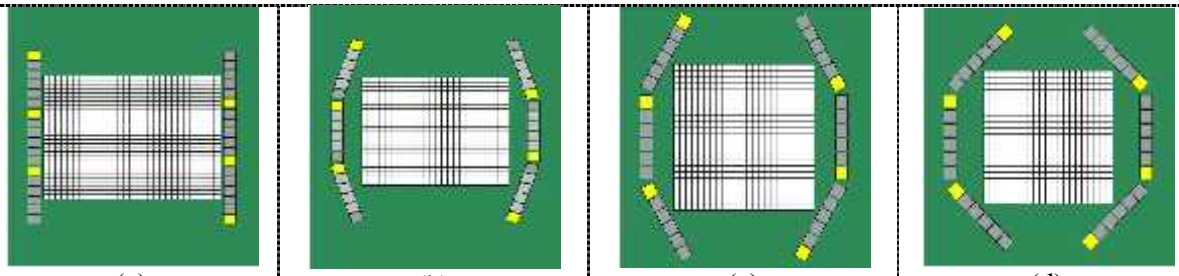

Figure 1. Illustration of the system configurations. (a) 0° (planar imaging), (b) 15°, (c) 30° and (d) 45° C-angle.

2.2. Phantoms

In order to evaluate the system's performance different phantoms were simulated. For the evaluation of the sensitivity and the FOV distortions two cylindrical water phantoms, were used. The phantoms were located in the center of the FOV and had diameters of 5 and 10 mm with a 1 MBq ^{18}F ion source.

For the evaluation of the spatial resolution we simulated capillary sources, with diameter of 1.1 mm, in an "L" arrangement. The location of the capillaries was at the center of the FOV (cap 1), 5 mm displaced on the X axis (cap 2) and 5 mm on the Y axis (cap 3). Each capillary was coupled to an ^{18}F source of 150 KBq. Other authors have presented different evaluation methods [17].

2.3. STIR reconstruction

The reconstructions were performed with STIR image reconstruction toolkit [18]. STIR does not support non-cylindrical geometries, out of the box. We had to calculate the system probability matrix (SPM) in advance and provide it as input to STIR during reconstruction. A modified Siddon ray tracer was implemented for this purpose [19].

For this initial investigation, the detectors were considered black, although the starting and ending point of the rays could be located in random places inside the crystal's volume. No inter-crystal scattering was taken into account.

3. Results and Discussion

3.1. Count rate performance

For the evaluation of the count rate performance of the system the cylindrical phantom, with diameter 10 mm, was used. The results showed (Figure 2) that the performance is improved with the C-angle, because the angular coverage is increased. From 0° to 45° the increase is approximately 15%.

3.2. FOV Distortion

In order to investigate the effect of the limited angular sampling the cylindrical phantoms with diameter 5 and 10 mm and C-angles 0° and 45°, were used. The results showed that in the

reconstructed images both phantoms were reconstructed distorted in some extent [20]. Along the X axis were enlarged and on the Y axis are slightly suppressed. The magnitude of the distortion effect depends on the size of the phantom and the C-angle.

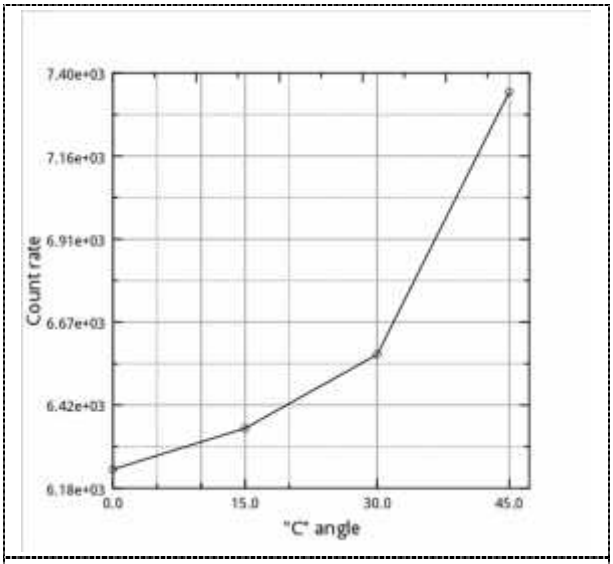

Figure 2. Count rate performance of the system over the C-angle.

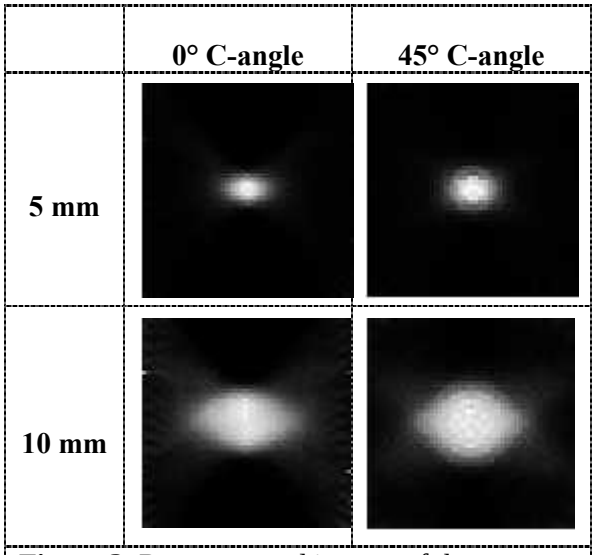

Figure 3. Reconstructed images of the two cylindrical phantoms with diameters 5 and 10 mm, for C-angles 0° and 45°

3.3. Spatial resolution

The spatial resolution results for 0º and 45 º C-angle, are presented. The results showed that for the 0° C-angle the distortion of cap 2 interfered with cap 0, rendering the measurement on X axis impossible. On the Y axis the two sources are distinguished but are slightly deformed with profiles of 1.7 mm and 1 mm, for cap 1 and cap 3, respectively.

From the 45° configuration, due to the improved angular coverage, the spatial resolution in all three locations, is 2 mm, both on X and Y axis. The spatial resolution on planar systems strongly depends on the crystal size of the detectors.

C-angle	Reconstructed image	Profile on X axis	Profile on Y axis
0°		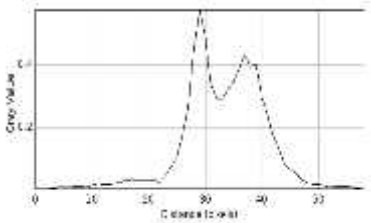	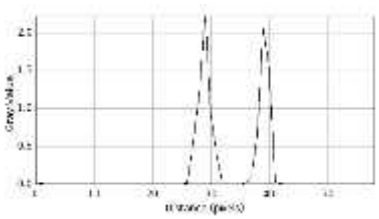
45°	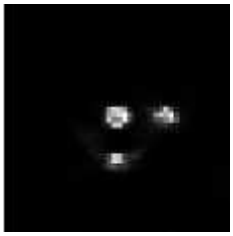	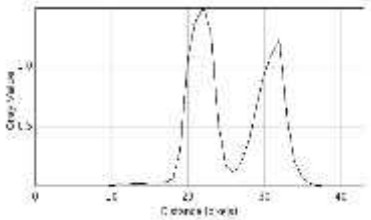	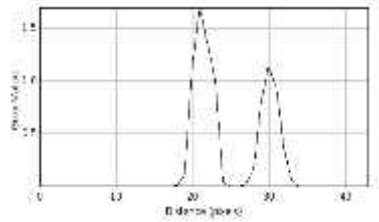

Figure 4. Reconstructed images after 4 iterations of three ^{18}F capillary sources, for C-angles 0° and 45° and the corresponding profiles on X and Y axis

4. Conclusions

Design considerations for a C-shaped PET system, dedicated to mouse brain imaging, were presented. The geometry was based on two opposite C-shaped heads. The C-angle of the heads was set to deferent values in order to investigate the impact on the sensitivity, distortions in the reconstructed image due to the limited angle sampling and spatial resolution.

It was found that the count rate performance of the system is improved for larger C-angles compared to planar head configuration, due to better angular coverage, on the expense of smaller images.

In addition, with larger C-angles the distortion in the FOV, due to the limited angle samples, is gradually reduced. The axis perpendicular to the heads is more sensitive to this effect. Other researched have also reported on this distortion and demonstrated that time of flight can eliminate them [20].

The spatial resolution of the system was found to be 2 mm, as the crystal size, when adequate angular sampling is achieved.

Acknowledgements

This research has been co-funded by the European Union (European Social Fund) and Greek national resources under the framework of the "ARISTEIA II" project HYPERGNOSTIC code 4309 of the "Education & Lifelong Learning" Operational Programme.

References

[1] Yu Ram A, Kim J S, Kang J H and Lim S M 2015 *J INST* **10**, P04001
[2] Kwon S I, Lee J S, Yoon H S, Mikiko I, Ko G B, Choi J Y et. al 2011 *J Nucl. Med.* **52**, 572
[3] Sanchez F, Orero A, Soriano A, Correcher C et. al. 2013 *Med. Phys.* **40** 051906
[4] Karpetas G E, Michail C M, Fountos G P, Kandarakis I S et. al. 2014 *Nucl. Med. Commun.* **35** 967
[5] Miranda-Menchaca A, Martinez-Davalos A, Murrieta-Rodriguez T, Sánchez-Alva H and Villafuerte-Rodriguez M 2015 *J INST* **10** T05008
[6] Islamirad S Z, Peyvandi R G, Lehdarboni M A and Ghafari A A 2015 *Nucl. Instr. Meth. Phys. Res. Sect. A* **781** 6
[7] Herraiz J L, Espana S, Cal-Gonzalez J, Vanquero J J, Desco M and Udias J M 2010 *Nucl. Instr. Meth. Phys. Res Sect A* **648** S169
[8] Efthimiou N, Maistros S, Tripolitis X, Samartzis A, Loudos G and Panayiotakis G 2011 *Meas. Sci. Tech.* **22** 114010
[9] Shao Y, Sun X, Lou K, Zhu X R et. al. 2014 *Phys. Med. Biol.* **59** 3373
[10] Zhang H, Bao Q, Vu N T, Silverman R W et.al. 2011 *Mol. Imag. Biol.* **13** 949
[11] Peng H 2015 *Nucl. Instr. Meth. Phys. Res. Sect.* A **779** 39
[12] Kao C-M, Dong Y and Chen C-T 2008 *IEEE Nucl. Sci. Symp. Conf. Rec.* M06-123
[13] David S, Georgiou M, Fysikopoulos E, Efthimiou N et. al. 2011 *IEEE Nucl. Sci. Symp. Conf. Rec.* 1886
[14] Raylman R R, Majewski S, Weisenberger A G and Popov V 2001 *J. Nucl. Med.* **42** 960
[15] Sarrut D, Bardiès M, Boussion N and Freud N 2014 *Med. Phys.* **41** 064301
[16] Valais I, Michail C, David S, Liaparinos P, Fountos G, Paschalis T, Kandarakis I and Panayiotakis G 2010 *IEEE Trans. Nucl. Sci.* **57**(1):3
[17] Karpetas G, Michail C, Fountos G, Valsamaki P, Kandarakis I and Panayiotakis G 2013 *Hell. J. Nucl. Med.* **16**(2) 111
[18] Thielemans K, Tsoumpas C, Mustafovic S, Beisel T, Anguiar P, Dikaios N and Jacobson M W 2012 *Phys. Med. Biol.* **57** 867
[19] Siddon R L 1984 *Med. Phys.* **12** 252
[20] Surti S and Karp J S 2008 *Phys. Med. Biol.* **53** 2911